Supplemental Information

Engineering Non-Hermitian Skin Effect with Band Topology in Ultracold Gases

Lihong Zhou, Haowei Li, Wei Yi, and Xiaoling Cui

In this Supplementary Information we provide the Raman transition diagram for a specific atomic candidate, the existence of non-Hermitian skin effect (NHSE) and band topology, and the lattice dynamics under realistic external confinements.

Supplementary Note 1:Detailed Raman-transition scheme for ^{173}Yb

We illustrate the implementation of our scheme, using level structures of ^{173}Yb atoms as a concrete example. In previous experiments with ^{173}Yb, both the optical Raman lattice [1] and 1D spin-orbit coupling (SOC) with dissipation (or the non-Hermitian SOC) [2] have been successfully implemented. The Raman transitions in these experiments are between the two hyperfine states in the ground-state $^1S_0$ manifold ($|\uparrow\rangle = |F = 5/2, m_F = 5/2\rangle$ and $|\downarrow\rangle = |F = 5/2, m_F = 3/2\rangle$), and the excited states with $F' = (7/2, 5/2, 3/2)$ states the $^3P_1$ manifold. The spin-dependent loss is controlled by a near-resonant transition from $|\downarrow\rangle$ to the excited state $|F', m'_F\rangle = |7/2, 1/2\rangle$. In view of these existing implementations, in Supplementary Figure 1 we show a specific Raman transition diagram based on the level structures of ^{173}Yb, for realizing our scheme in Fig. 1(a) of the main text.

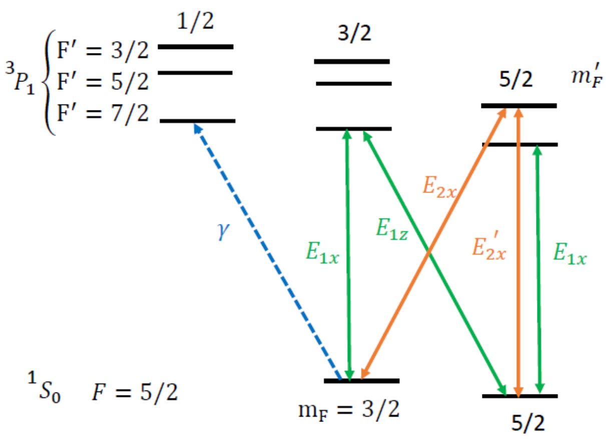

Supplementary Figure 1: (Color online) A proposed Raman-transition diagram for ^{173}Yb.

Here the choice of two spin states $|\uparrow, \downarrow\rangle$, and the energy levels to create the optical Raman lattice, the M_0-SOC and the spin-dependent loss are all consistent with [1, 2]. To ensure an independent control on the M_r-SOC (from the M_0-SOC), we propose to consider the Raman transition to a different excited state, say, $|F', m'_F\rangle = |5/2, 5/2\rangle$, as shown in Supplementary Figure 1. A specific atomic transition can be achieved by tuning the laser frequency via the acousto-optical modulater (AOM) to exactly match the required atomic energy difference.

Supplementary Note 2:Non-Hermitian skin effect and band topology in the general (ϕ_r, ϕ_0) phase plane

Here we discuss the presence of NHSE and band topology in case-III with general phase parameters (ϕ_r, ϕ_0).

First, we discuss the band topology when the system is away from the points $(\phi_r = \pi, \phi_0 = \pi/2, 3\pi/2)$. In Supplementary Figure 2, we show the OBC spectrum by taking the same $(\Omega_0, \Omega_r, \gamma)$ as those in Fig. 3 of the main text, but with two different sets of phase parameters (ϕ_r, ϕ_0). We see that the topological zero modes are now replaced by two finite-energy in-gap modes.

To gain more insight to the vanishing of the topological zero modes under OBC, let us examine the Bloch Hamiltonian $H(k)$ for $\phi_r = \pi$ and $\phi_0 \neq \pi/2, 3\pi/2$. In this case, $H(k)$ develops a σ_y component,

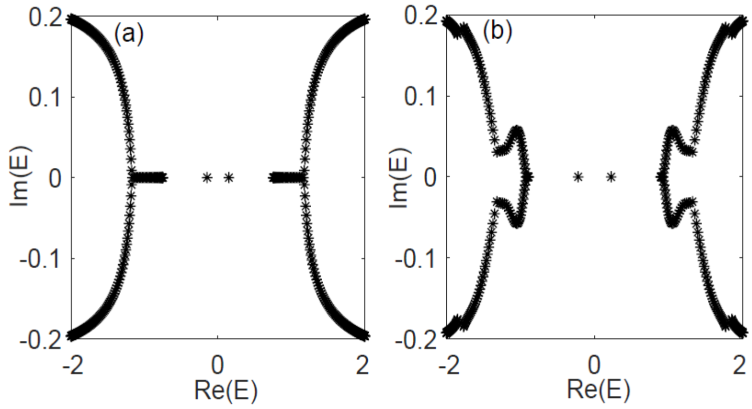

Supplementary Figure 2: Energy spectrum under the open boundary condition (OBC) for (a) $(\phi_r, \phi_0) = (\pi, \pi/3)$ and (b) $(\phi_r, \phi_0) = (2\pi/3, \pi/2)$. In both cases we take $\Omega_0 = 0.5, \Omega_r = 0.3, \gamma = 0.2$, the same as in Fig. 3 of the main text. The energy unit is taken as hopping t.

and the chiral symmetry is no longer present. We have also verified from the tight-binding model that the chiral symmetry breaks down also for $\phi_r \neq \pi$, and thus the band topology is destroyed as long as (ϕ_r, ϕ_0) deviates from the points $(\pi, \pi/2)$ and $(\pi, 3\pi/2)$.

Finally, the appearance of the NHSE is found to be much more robust as compared to the band topology. We have explained in the main text that for the case $\phi_r = \pi$, the skin effect can hold for all ϕ_0 except for $\phi_0 = 0, \pi$. For other $\phi_r \neq \pi$, we have numerically checked the energy spectrum under PBC and the eigen-modes under OBC, and conclude that the skin effect can expand to all the phase parameters except for $\phi_r = 0$. In fact, for $\phi_r = 0$, we can write down the tight-binding Hamiltonian in the k space as

$$\begin{aligned} H = &-\sum_k 2t\cos k(c^\dagger_{k\uparrow}c_{k\uparrow} - c^\dagger_{k\downarrow}c_{k\downarrow}) + i\gamma\sum_k(c^\dagger_{k\uparrow}c_{k\uparrow} - c^\dagger_{k\downarrow}c_{k\downarrow}) \\ &+ \Omega_0\sum_k(-ie^{i\phi_0}2\sin k c^\dagger_{k\uparrow}c_{k\downarrow} + H.c.) + \Omega_r\sum_k(c^\dagger_{k\uparrow}c_{k-\pi,\downarrow} + H.c.). \end{aligned} \tag{1}$$

We see that the last term couples k to $k-\pi$, and in the basis $\psi = (c_{k-\pi,\uparrow}, c_{k-\pi,\downarrow}, c_{k,\uparrow}, c_{k,\downarrow})^T$, we have $H = \sum_k \psi^\dagger h(k)\psi$ with $h(k)$ a 4×4 matrix. The diagonalization of $h(k)$ gives rise to the eigen-spectrum under PBC. In Supplementary Figure 3, we show two typical energy spectra in the complex energy plane for $\gamma < \Omega_r$ and $\gamma > \Omega_r$ with $\phi_0 = \pi/2$. We see that the PBC spectrum in the complex plane behaves either as two disconnected lines or as two open arcs, but not closed loops. Other ϕ_0 cases shows similar features. Therefore the NHSE does not show up if $\phi_r = 0$.

In Supplementary Figure 4 we summarize the existence regions for the NHSE for case-III in the phase plane (ϕ_r, ϕ_0). It is shown that the skin effect is absent for two discrete points $(\pi, 0)$ and (π, π) and a line at $\phi_r = 0$.

Supplementary Note 3:Non-Hermitian skin effect under realistic confinements

Here we consider two types of realistic confinements in cold atoms, one is the box-trap potential with clear edges, and the other is the harmonic potential without a clear edge. In the first case, we consider the realistic situation when the edge is not sharp enough, i.e., there is an additional large but finite laser potential on each side of the lattice, see the illustration in Supplementary Figure 5(a). To examine the effect of edge imperfection, we have computed the edge-to-edge transport from

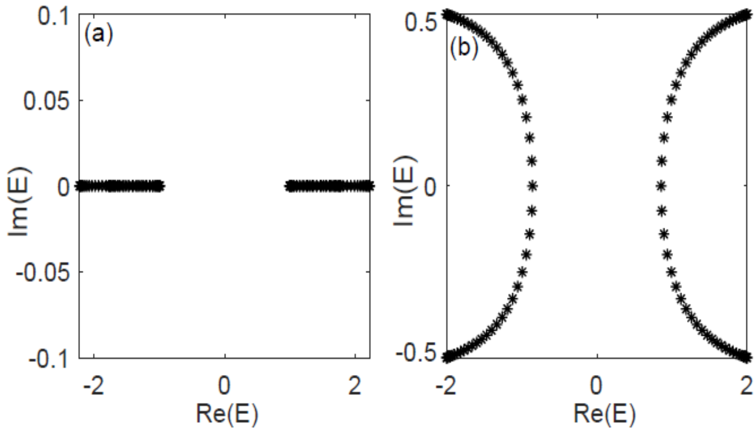

Supplementary Figure 3: Energy spectrum under periodic boundary condition (PBC) for (a) $\Omega_0 = 0.5, \Omega_r = 0.3, \gamma = 0.2$ and (b) $\Omega_0 = 0.5, \Omega_r = 0.3, \gamma = 0.6$. In both cases we take $(\phi_r, \phi_0) = (0, \pi/2)$. The energy unit is taken as hopping t.

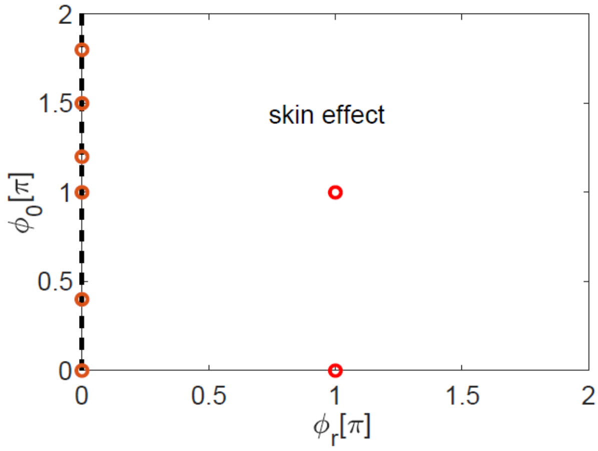

Supplementary Figure 4: (Color online) The region of non-Hermitian skin effect(NHSE) in the plane of (ϕ_r, ϕ_0). The red circles at $(\pi, 0)$ and (π, π), as well as the dashed line at $\phi_r = 0$, denote the parameter regimes for the absence of the non-Hermitian skin effect. The energy unit is taken as hopping t.

$i = 1$ to L (P_{LR}) or from $i = L$ to 1 (P_{RL}), when the laser potentials are applied at sites $i = 0$ and $L + 1$ with strength V. For simplicity, in our numerics the hopping rate between different sites and all other parameters are taken to be the same as those without the box potential. The results are shown in Supplementary Figure 5 ((b)i,(b)ii) for $V = 5t$.

For the first case, we see that the edge-to-edge transport shares qualitatively the same features as those in Fig. 5 of the main text. In the topological phase without NHSE (Supplementary Figure 5((b)i)), P_{LR} and P_{RL} are identical to each other, and the oscillation frequency decays exponentially with size L. In comparison, the dynamics with NHSE shows obvious directional preference (Supplementary Figure 5((b)ii)), as the localized bulk states contribute significantly.

We now turn to the second case and discuss the manifestation of NHSE in a lattice system under a harmonic trap, $V(x) = V_0 x^2$, where the edge is not well-defined. In our simulation, we take the trap center at the lattice site i_0 and thus there is a local on-site potential $\mu_i = V(i - i_0)^2$ to each site index i, with $V = V_0 a^2$ (a is the lattice spacing). We then consider the expansion dynamics of a particle from the trap center $i = i_0$, see illustration in Supplementary Figure 6(a). To eliminate the difference caused by spin, we consider the initial state as an equal population of $|\uparrow\rangle$ and $|\downarrow\rangle$ at

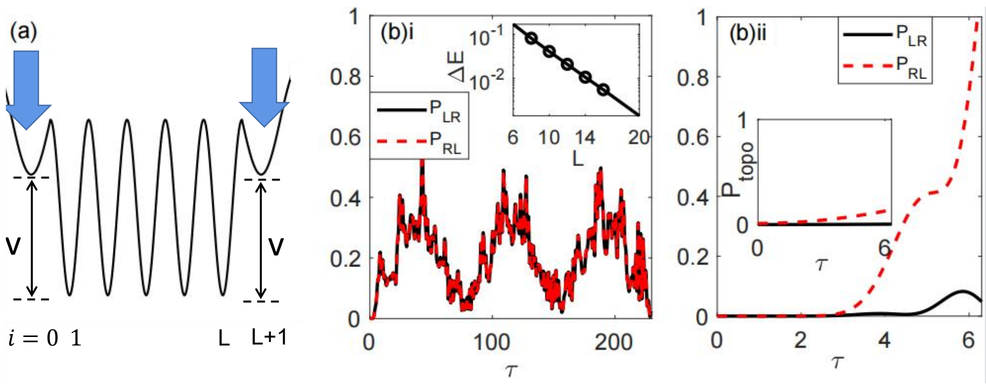

Supplementary Figure 5: (Color online) (a) Illustration of the lattice system under a box potential with imperfect edges. ((b)i, (b)ii) P_{LR} and P_{RL} between lattice sites $i = 1$ and L without ((b)i) and with ((b)ii) non-Hermitian skin effect(NHSE). Here we take the laser potential $V = 5t$, and all other parameters are identical to Fig. 5 in the main text. The insets of ((b)i) and ((b)ii) are also the same physical quantities as in the insets of Fig. 5 in the main text. The energy unit is taken as hopping t, and the time unit is $\hbar/t$.

site i_0, and then examine the probability of finding a particle at site n after an evolution time of τ, defined as

$$\rho_n(\tau) \equiv \sum_{\sigma} |\psi_{n,\sigma}(\tau)|^2. \tag{2}$$

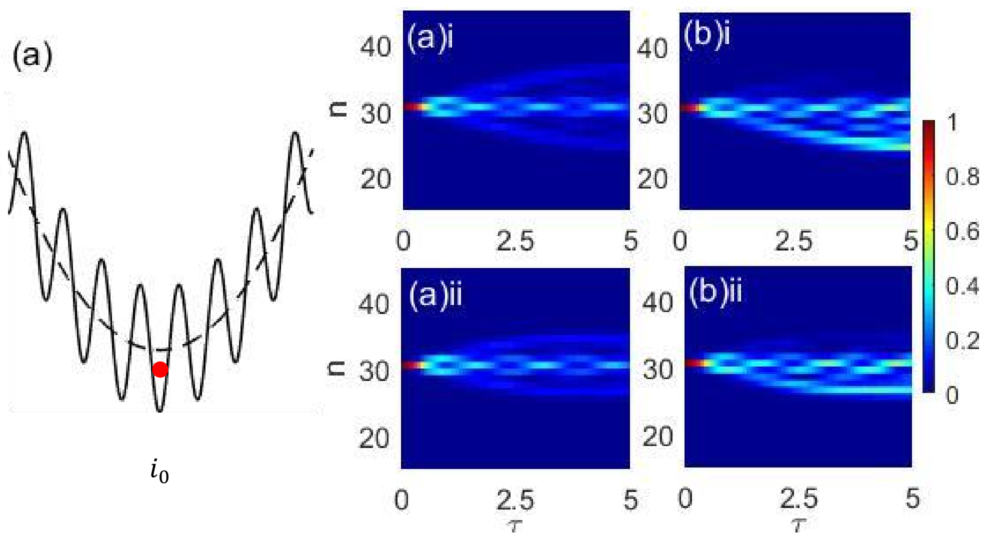

Supplementary Figure 6: (Color online) (a) Illustration of the lattice system with an additional harmonic potential. ((a)i,(a)ii,(b)i,(b)ii) Contour plot of $\rho_n(\tau)$ in the (n, τ) plane for the bulk dynamics in a harmonic trap. Here we take $\Omega_r = 1, \Omega_0 = 0.5$, and other parameters are $(\gamma, V) = (0, 0.1)$((a)i), $(0.2, 0.1)$((b)i), $(0, 0.2)$((a)ii), $(0.2, 0.2)$((b)ii). The lattice size is $L = 60$, and the particle is initialized at $i_0 = L/2$ (the trap center). The energy unit is taken as hopping t, and the time unit is $\hbar/t$.

In Supplementary Figure 6((a)i,(a)ii,(b)i,(b)ii), we show the contour plot of $\rho_n(\tau)$ in the (n, τ) plane for various cases of γ and V parameters. One can see that in the absence of NHSE ($\gamma = 0$ in ((a)i,(a)ii)), the particle wave function expands from the trap center with equal probabilities to the right- and left-hand sides. In comparison, when the NHSE is present under a finite γ ((b)i,(b)ii), the expansion shows strong directional preference towards the left-hand side (smaller index) of the lattice. The probability peak apparently moves to the left-hand side of the trap center at short times, which then saturates at a certain distance to the trap center at longer times. By comparing ((a)i,(a)ii) and ((b)i,(b)ii) with different harmonic confinements, we can see that a stronger V will suppress the directional flow, i.e., the off-center displacement of the particle becomes smaller as V increases, whereas the off-center accumulation of population becomes more appreciable. We have also checked that in the absence of the harmonic trap $V = 0$, the expansion peak moves to left-hand side continuously (before getting close to any boundaries). These results show that even there is no sharp edge or boundary, the NHSE can also manifest itself in the bulk dynamics.

Supplementary References

[1] B. Song, L. Zhang, C. He, T. F. Jeffrey Poon, E. Hajiyev, S. Zhang, X.-J. Liu, G.-B. Jo, "Observation of symmetry-protected topological band with ultracold fermions", Sci. Adv. 4, eaao4748 (2018).

[2] Z. Ren, D. Liu, E. Zhao, C. He, K. K. Pak, J. Li, G.-B. Jo, "Topological control of quantum states in non-Hermitian spin-orbit-coupled fermions", arxiv: 2106.04874; Nat. Phys. (2022). https://doi.org/10.1038/s41567-021-01491-x